GEOPHYSICAL RESEARCH LETTERS, VOL. 24, NO. 21, PAGES 2541-2544, NOVEMBER 1, 1997

Observations of the Ekman balance at 8°30′ N in the Arabian Sea during the 1995 southwest monsoon

T. K. Chereskin,[1] W. D. Wilson,[2] H. L. Bryden,[3] A. Ffield,[4] and J. Morrison[5]

Abstract. The Ekman transport is estimated from two sets of hydrographic and shipboard acoustic Doppler current profiler (ADCP) velocity observations made during June and September 1995, during the southwest monsoon in the Arabian Sea. Both sets of measurements were made along latitude 8°30′ N, designated as World Ocean Circulation Experiment (WOCE) line I1W, from Somalia to Sri Lanka. The Ekman transport estimates calculated from ageostrophic velocity were southward: 17.6±2.4 10^6 m^3 s^{-1} in June and 7.9±2.7 10^6 m^3 s^{-1} in September. These direct estimates were in good agreement with those predicted by the Ekman balance using both shipboard and climatological winds. The vertical structure of the ageostrophic velocity and the stratification were quite different between the two occupations of the transect. The wind-driven momentum was confined to a very shallow layer in June (about 50 m) and the surface layer was strongly stratified, with a maximum salinity layer at depths between 50 and 70 m. The ageostrophic velocity penetrated much deeper in September (to about 160 m) and the pycnocline was correspondingly deeper. In both cases, the Ekman transport penetrated beneath the mixed layer, to the top of the pycnocline.

Introduction

Ekman [1905] proposed a balance of forces in the surface layer between a steady wind stress and the Coriolis force, resulting in an anticyclonic velocity spiral with depth and a net surface layer transport at right angles to the wind direction. Integrated across an ocean basin, the Ekman transport can be several tens of Sverdrups (1 Sv = 10^6 m^3 s^{-1}). Strong, quasi-steady wind forcing at low latitudes produces particularly large wind-driven transports: a direct estimate at 11°N in the Atlantic Ocean is 12±5.5 Sv [*Chereskin and Roemmich,* 1991] and a direct estimate at 10°N in the Pacific, along a section roughly four times the length of the Atlantic transect, is 62±10 Sv [*Wijffels et al.,* 1994]. The Ekman transport is thus an important component of the flow, and some estimate of it is required in order to close the mass budget prior to estimating oceanic heat and property fluxes. Since the Ekman transport is not usually directly observed, it is most often estimated from wind stress climatology. Two disadvantages of estimating the Ekman transport from climatology are the uncertainty of whether climatological winds are representative of a particular period and the unresolved Ekman contribution to heat and property fluxes since its vertical structure (maximum depth of penetration) is unknown.

The Arabian Sea is an ideal location for the study of wind-driven flows. Its circulation is dominated by two monsoons – the southwest monsoon in boreal summer and the northeast monsoon in winter. Winds are strong and steady during the monsoons, weak and variable between them. A prominent feature of the monsoons is the development of a strong, persistent, low-level atmospheric jet. During the southwest monsoon, a southwesterly jet forms over the Somali coast sometime in April or May and extends out over the Arabian Sea in June (Figure 1). Peak winds usually occur in July, and the monsoon generally persists through September. The 1995 southwest monsoon followed this pattern

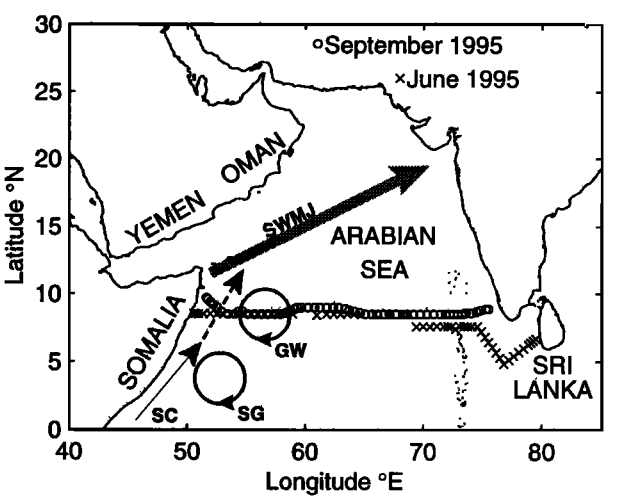

Figure 1. Ship tracks and locations of hydrographic stations. The southwest monsoon jet (SWMJ), the Somali Current (SC), the Great Whirl (GW), and the Southern Gyre (SG) locations are shown schematically.

[1]Scripps Institution of Oceanography, University of California, San Diego.
[2]Atlantic Oceanographic and Meteorological Laboratory, Miami, Florida.
[3]Southampton Oceanography Centre, United Kingdom.
[4]Lamont-Doherty Earth Observatory, Palisades, New York.
[5]North Carolina State University, Rayleigh, North Carolina.

Copyright 1997 by the American Geophysical Union.

Paper number 97GL01057.
0094-8534/97/97GL-01057$05.00

[*Rudnick et al.*, 1997]. Associated with the atmospheric jet is the Somali Current, a strong (speeds > 1 m s^{-1}), surface-intensified (upper 400 m), seasonally reversing boundary current off Somalia. As the southwest monsoon intensifies, the Somali Current penetrates northward, crossing the equator typically in May and 10°N in late August [*Schott et al.*, 1990]. The recirculation gyres known as the Great Whirl and Southern Gyre also usually develop (Figure 1). *Schott et al.* [1990] estimated the average summer transport of the Somali Current at the equator to be 21 Sv northward, using moored current estimates made in the upper 500 m, from the coast out to 180 km offshore. At 8–10°N, the Somali Current is augmented by the Great Whirl, and northward transports are 2-3 times this amount, but much of the additional transport recirculates locally [e.g., *Fischer et al.*, 1996]. At 8°30′ N, any net northward boundary current flow must be balanced by southward flow at the same latitude because the Arabian Sea forms essentially a closed basin north of 8°N. Air-sea heat exchange, high evaporation rates, intense biological productivity, and upwelling within the Arabian Sea during the southwest monsoon all imply property transformations. In addition to being a source of salt, the Arabian Sea is a biological "pump" during the monsoons, and the Ekman heat, freshwater, and nutrient fluxes are important components of a meridional overturning cell. To determine the net exchange of properties between the Arabian Sea and the Indian Ocean, it is critical to identify the vertical partitioning of the meridional flow across latitude 8°30′ N.

The purpose of this letter is twofold. First, we compare direct estimates of Ekman transport in June and September 1995 across latitude 8°30′ N in the Arabian Sea to the Ekman tranports predicted by the wind. We are aware of only two such direct estimates across the width of an ocean basin: in the tropical Atlantic and Pacific [*Chereskin and Roemmich*, 1991; *Wijffels et al.*, 1994] where the Trade winds force a northward transport in the surface layer. In the Arabian Sea, the seasonally reversing monsoon is responsible for a seasonally reversing Ekman transport, southeastward during the southwest monsoon and northwestward during the northeast monsoon. The second goal of our letter is to describe and compare the vertical structure of the wind-driven flow, which was quite different between our two occupations of the section. The total top-to-bottom heat, salt, and property fluxes across 8°30′ N are the subject of future work.

Method

In the northern hemisphere, the Ekman transport relation predicts a net transport to the right of the surface wind stress, τ_0,

$$\int_{-H}^{0} v_E dz = \frac{\tau_0}{\rho f}, \qquad (1)$$

where the Coriolis parameter f is twice the vertical component of the earth's rotation vector, ρ is the water density, v_E is the ageostrophic velocity component to the right of the wind direction, and H is the maximum depth of penetration of the wind stress.

We estimated the Ekman transport across two transects made from Somalia to Sri Lanka from the R/V Baldridge (June 5–19, 1995) and R/V Knorr (September 12–26, 1995). Both transects consisted of 56 conductivity-temperature-depth (CTD) stations, spaced approximately every 60 km in mid-ocean and more closely at the boundaries (Figure 1). Shipboard ADCP velocity observations and vector wind measurements were made continuously along the ship tracks. The calculation follows that of *Chereskin and Roemmich* [1991], which we summarize briefly below.

Vector-averaged winds were computed for the underway intervals between CTD stations. *Large and Pond's* [1981] bulk formulas, which provide speed-dependent drag coefficients, were used to compute wind stress, assuming a neutrally stable atmospheric boundary layer. A comparison of the along-track (eastward) stress calculated from shipboard winds to climatological winds for June and September [*Hellerman and Rosenstein*, 1983] (hereafter HR) is shown in Figure 2. HR stress was linearly interpolated to 8°30′N. The wind-based estimates of Ekman transport are calculated from the along-track integral of the along-track wind stress for each section,

$$\int_{50^\circ E}^{77^\circ E} \frac{\tau_0}{\rho f} dx. \qquad (2)$$

Both the ADCP and the CTD data provide estimates of current shear rather than absolute current. We estimated the ageostrophic shear as the difference between the total current shear measured by the shipboard ADCP and the geostrophic shear. The geostrophic shear was calculated between each CTD station pair, and the total shear was averaged over the same interval. In each case, the velocities were referenced to

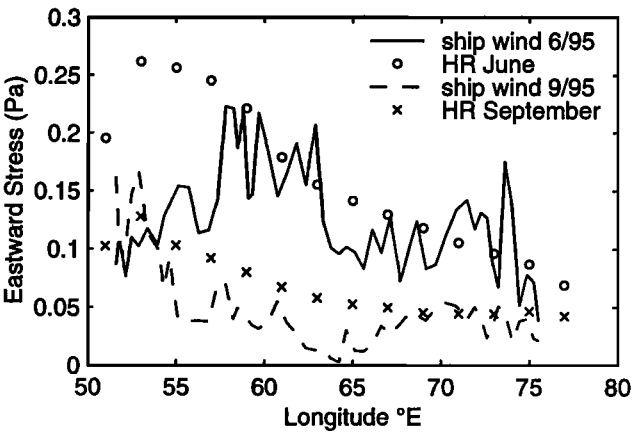

Figure 2. Comparison of in-situ shipboard wind stress and Hellerman-Rosenstein climatological stress for June and September.

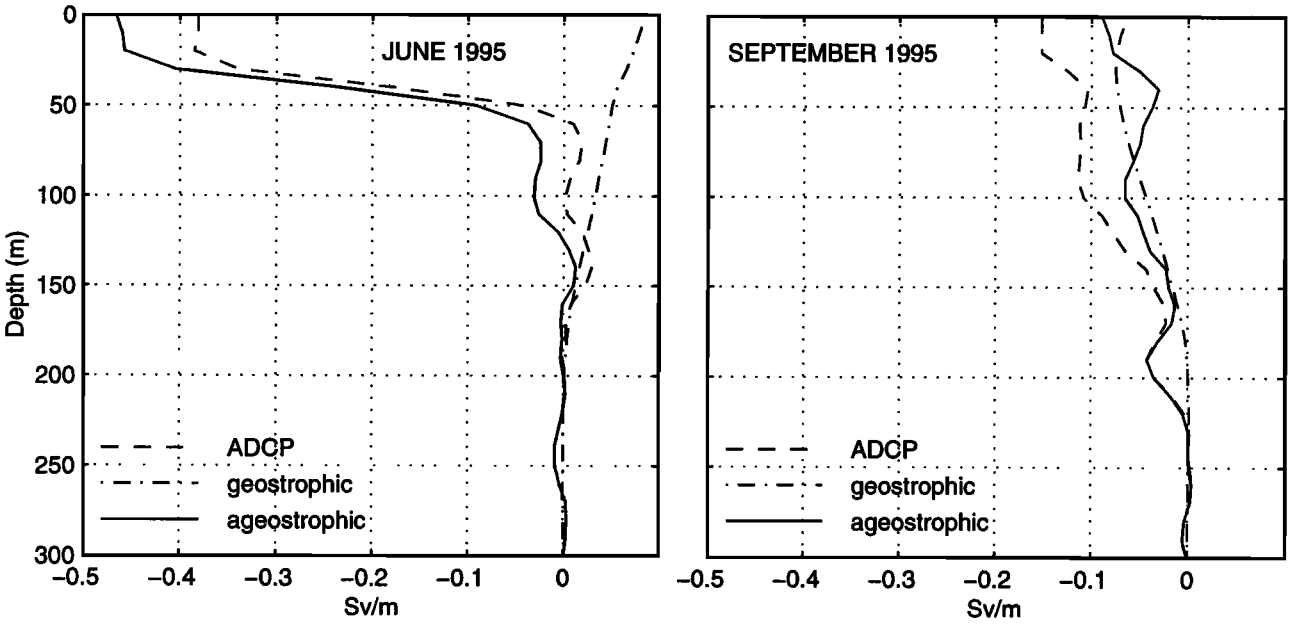

Figure 3. Transport per unit depth. Units are 10^6 m^2s^{-1} (Sv/m).

300 m, a depth far below the mixed layer and the maximum depth of direct wind influence. The key assumption is that the ageostrophic flow is surface intensified and vanishes at 300 m. The total flow is assumed to be in geostrophic balance at 300 m. Above 20 m, the shallowest depth sampled by the ADCP, the velocity was assumed constant.

The direct estimates of Ekman transport are calculated from the along-track integral of the cross-track ageostrophic velocity along each section (the transport per unit depth, Figure 3), integrated vertically from the surface to the maximum depth of penetration of the wind stress.

$$\int_{-H}^{0}\int_{50^\circ E}^{77^\circ E} v_{ageos}\,dx\,dz. \qquad (3)$$

Table 1 summarizes the Ekman transport estimates. Sensitivity of (3) to the choice of H is discussed below.

Discussion and Summary

Overall, there is excellent agreement between our direct and wind-based estimates of Ekman transport. The shipboard estimates indicated about 18 Sv southward Ekman transport in June and about 7 Sv southward in September. The climatological stress predicted somewhat larger values, about 23 and 10 Sv southward, respectively. The climatological stress is much smoother than the section snapshots (Figure 2). In June 1995, the stress was anomalously low relative to HR at the western boundary, and in September 1995, the mid-basin stress was low relative to HR. In assigning an error bar to the wind-based estimates, we assumed that the 20% uncertainty in the drag coefficient [*Large and Pond,* 1981] was the dominant error source. Error bars on the ageostrophic estimate were calculated as in [*Chereskin and Roemmich,* 1991] using a bootstrap algorithm [*Efron and Tibshirani,* 1993].

There is a striking difference in the vertical distribution of the ageostrophic transport between June and September (Figure 3). In each case, there is a surface maximum that we identify as the Ekman flow. The maximum decays with depth to a minimum at about 160 m, the depth used for calculating (3). In June almost all the transport (-17.3 Sv) was confined within a very sharply defined layer between the surface and 50 m; integrating to any deeper level did not change the total transport by more than 1 Sv. In contrast, the September transport, about half of the June value, extended about three times as deep. The transport in the top 50

Table 1. Ekman Transport Estimates

	Ageostrophic[1]	Ship Wind	HR Wind[2]
June	-17.6 ± 2.4	-19.1 ± 3.8	-22.7 ± 4.5
September	-7.9 ± 2.7	-6.4 ± 1.3	-9.6 ± 1.9

[1]integrated from the surface to 160 m
[2]*Hellerman-Rosenstein* [1983] climatological wind stress

m was only about -3 Sv. There is a small maximum in ageostrophic velocity below 160 m in September that is associated with deep ageostrophic flow near 55°E, in the Great Whirl. It is excluded from the integral because it is probably not due to wind forcing. Ageostrophic non-Ekman flows are the principal source of uncertainty in the ageostrophic estimate of the Ekman transport. Integrating below 160 m did not change the September transport by more than 1.5 Sv.

The stratification was also quite different between the two occupations of the section. The surface layer was warmer in June than September, and a subsurface salinity maximum extended across much of the section, in the depth range from 50 to 70 m, beneath the bulk of the Ekman transport. In September, the salinity maximum layer extended to the surface in mid-basin, and the mean depth of the layer was deeper ($\approx$ 100 m) than in June. These differences between June and September, the monsoon onset and end, are consistent with climatology [*Levitus et al.*, 1994] and suggest quite different Ekman heat and salt fluxes for the two periods.

The horizontal distribution of the ageostrophic flow (i.e., the station pairs) followed the pycnocline pattern, with much deeper penetration in the west, where the pycnocline was deeper and the winds were stronger. We defined the mixed layer as the depth where the density increased by 0.01 kg m^{-3} from its surface value and the top of the pycnocline as the depth at which the density gradient increased by 0.01 kg m^{-4}. The mean mixed layer depth was quite shallow in both June and September, about 10 m, and fairly uniform across the sections. The depth of the pycnocline, however, was quite different: mean top of the pycnocline in June was 15 m (with a range of 100 to 10 m), and the mean in September was 78 m (with a range from 220 m to 10 m). The pycnocline sloped upward from west to east, and as the range numbers indicate, the slope was more pronounced in September, with a much deeper pycnocline at the western boundary than in June.

The penetration of the wind-driven flow beneath the mixed layer, to the top of the pycnocline, appears to be a common feature of direct observations of the Ekman transport; it was also observed in the Atlantic and Pacific [*Chereskin and Roemmich*, 1991; *Wijffels et al.*, 1994]. The deep penetration means that the Ekman layer advects water below the mixed layer. Thus, the Ekman contribution to the heat and salt fluxes must be measured; it can not be determined merely by inferring the volume transport from the wind and using the surface temperature and salinity. The Ekman heat and salt fluxes and their contribution to the total fluxes are the subjects of our continuing investigations.

Acknowledgments. The Knorr and Baldridge transects were supported by the National Science Foundation (NSF) and the National Oceanic and Atmospheric Administration (NOAA), respectively. We thank the anonymous reviewers for improving the manuscript and A. J. Harding for useful comments and help with the figures. Support from the following grants is acknowledged: NSF OCE92-16411 and OCE94-13174 (TKC), NSF OCE94-1316 (HLB and JM), and NOAA NA66GP0267 (AF). HLB's participation was also supported by the Natural Environment Research Council under the WOCE special topic. WDW was partially supported by a grant from the NOAA Office of Global Programs.

References

Chereskin, T. K., and D. Roemmich, A comparison of measured and wind-derived Ekman transport at 11°N in the Atlantic Ocean, *J. Phys. Oceanogr.*, *21*, 869-878, 1991.

Efron, B., and R. J. Tibshirani, *An Introduction to the Bootstrap*, 436 pp., Chapman and Hall, New York, 1993.

Ekman, V. W., On the influence of the earth's rotation on ocean-currents, *Ark. Mat. Astron. Fys.*, *2*, 1-52, 1905.

Fischer, J., F. Schott, and L. Stramma, Currents and transports of the Great Whirl-Socotra Gyre system during the summer monsoon, August 1993, *J. Geophys. Res.*, *101*, 3573-3587, 1996.

Hellerman, S., and M. Rosenstein, Normal monthly wind stress over the world ocean with error estimates, *J. Phys. Oceanogr.*, *13*, 1093-1104, 1983.

Large, W. G., and S. Pond, Open ocean momentum flux measurements in moderate to strong winds, *J. Phys. Oceanogr.*, *11*, 324-336, 1981.

Levitus, S., R. Burgett, and T. Boyer, World Ocean Atlas 1994, *NOAA Atlas NESDIS*, *3*, U.S. Department of Commerce, Washington, D.C., 1994.

Rudnick, D. L., R. A. Weller, C. C. Eriksen, T. D. Dickey, J. Marra, and C. Langdon, Moored instruments weather Arabian Sea monsoons, yield data, *Eos Trans. AGU*, *78*,, 117, 1997.

Schott, F., J. C. Swallow, and M. Fieux, The Somali Current at the equator: annual cycle of currents and transports in the upper 1000 m and connection to neighbouring latitudes, *Deep Sea Res., Part A*, *37*, 1825-1848, 1990.

Wijffels, S., E. Firing, and H. Bryden, Direct observations of the Ekman balance at 10°N in the Pacific, *J. Phys. Oceanogr.*, *24*, 1666-1679, 1994.

T. Chereskin, Scripps Institution of Oceanography, University of California-San Diego, La Jolla, CA, 92093-0230. (e-mail: tchereskin@ucsd.edu)

W. Wilson, Atlantic Oceanographic and Meteorological Laboratory, Miami, FL, 33124. (e-mail: wilson@wdw.aoml.erl.gov)

H. Bryden, Southampton Oceanography Centre, Southampton, S014 3ZH U. K. (email: h.bryden@soc.soton.ac.uk)

A. Ffield, Lamont-Doherty Earth Observatory, Palisades, NY, 10964. (e-mail: affield@ldeo.columbia.edu)

J. Morrison, North Carolina State University, Rayleigh, NC, 27695. (e-mail: j_morrison@ncsu.edu)

(Received January 17, 1997; revised March 24, 1997; accepted March 31, 1997.)